

WALL PRESSURE FLUCTUATIONS IN SEPARATED AND REATTACHING FLOWS OVER A BACKWARD-FACING STEP

Inwon Lee

Department of Mechanical Engineering
Korea Advanced Institute of Science and Technology
373-1, Kusong-dong, Yusong-ku, Taejon, 305-701
South Korea

Hyung Jin Sung

Department of Mechanical Engineering
Korea Advanced Institute of Science and Technology
373-1, Kusong-dong, Yusong-ku, Taejon, 305-701
South Korea

ABSTRACT

Measurements were made of the wall pressure fluctuations in separated and reattaching flows over a backward-facing step. A new type of an array of pressure sensors, composed of PVDF (polyvinylidene fluoride), was employed to measure the spatio-temporal features of wall pressure field. Distributions of the root-mean-square (rms) pressure fluctuations as well as the pressure spectra and coherence of the surface pressure field were measured at various locations near the reattachment region. The experimental results showed that the level of fluctuating pressure rises rapidly in the downstream direction, reaching a maximum value near reattachment. As the reattached flow convects downstream, the low frequency content of the pressure spectrum decreases and the high frequency increases. A large-scale, convective spatial structure undergoes a relaxation process, evolving from its highly energized state at reattachment back toward an equilibrium.

INTRODUCTION

Surface pressure fluctuations are closely correlated with flow unsteadiness and aerodynamic noise generation in the immediate vicinity of the wall. A knowledge of this quantity is of prime importance in understanding the dynamic behavior of complex turbulent flows and flow noise. Much attention has been given to the accurate measurement of wall pressure fluctuations in the frequency and time domain. Most of previous studies have been concentrated on the investigation of spatial and spectral features of wall pressure fluctuations beneath turbulent boundary layers. (Choi and Moin, 1990; Farabee and Casarella, 1991; Schewe, 1983).

A literature survey reveals that, however, researches are not numerous which report measurements of the wall pressure fluctuations produced by turbulent separated and reattaching flows. Mabey (1972) compiled the rms

distribution and autospectrum of pressure fluctuations in various separated and reattaching flows. He suggested scaling method for the correlation of existing data sets. Recently, Govinda Ram and Arakeri (1990) measured the rms distribution of pressure fluctuations in flows over blunt bodies of various nose shapes.

The presence of flow separation, together with consecutive reattachment, gives rise to intense pressure fluctuations, thereby generating flow-induced structural vibrations and noise in many engineering applications. A canonical flow pattern over a backward-facing step indicates the formation of a separation as well as the emergence of reattached flow further downstream; see Eaton and Johnston (1981) for comprehensive review on global flow characteristics. The measurements which were conducted by Kiya and Sasaki (1983, 1985) and Cherry et al. (1984) exemplifies the large-scale coherent motion, where the scale is as large as several step heights. Therefore, in order to secure detailed information of pressure behavior in the frequency and wavenumber domain, it is highly desirable to employ multiple-arrayed pressure sensor which covers large streamwise extent.

A perusal of the relevant studies indicates that few studies of the spatio-temporal characteristics of pressure fluctuations in separated and reattaching flows have been made. Furthermore, the multiple-arrayed sensor applications in this area are very scarce. Most notable exception is the study by Farabee and Casarella (1986), who made measurement of coherence function and convection velocity of pressure fluctuations in the flow over a backward-facing step. But, as will be shown later, due to the limited number and array size of microphones, they could not resolve large-scale coherent motion.

Recently, toward the end of measuring the distribution of wall pressure fluctuations, Lee and Sung (1999) developed a

promising array of pressure sensors, which is composed of PVDF (polyvinylidene fluoride). This sensor has many advantages over conventional pressure-hole mounted transducers, one of which is the disturbance-free measurement of wall pressure fluctuations at relatively low price.

In the present study, wall pressure fluctuations in the flow over a backward-facing step are measured by utilizing the PVDF sensors. Values of the rms pressure fluctuations as well as frequency spectra are evaluated. The cross correlation coefficient and the coherence function of pressure fluctuations are also presented. The inhomogeneity of the flow field has been taken into consideration. Spatial and spectral characteristics of the wall pressure fluctuations are scrutinized.

EXPERIMENTAL APPARATUS

Wind tunnel and velocity measurement

A subsonic open-circuit wind tunnel, which was constructed in the earlier work of Chun and Sung (1996), was slightly modified for the present experiment. The settling chamber, honeycomb and screens were placed in sequence. Smooth contraction fairing with a large contraction ratio (6:1) and flow-conditioning elements (honeycomb and three screens) in the settling chamber ensured high-quality flow in the test section. The inlet channel had dimensions of 630 mm in width, 100 mm in height and 1000 mm in length. A trip wire was installed at the entrance of the inlet channel to make the inlet flow to be a fully turbulent. Air was driven by a centrifugal fan and 5HP-motor. The velocity in the test section was controlled by an inverter. The free-stream turbulence intensity was less than 0.6% at speeds $4.0 \leq U_0 \leq 14.0$ m/sec. No significant peaks were found in the spectrum of velocity fluctuations in the main flow.

The test section was a constant area rectangle duct whose dimension is 630 mm in width, 150 mm in height, and 2500 mm in length as shown. The step height H of a backward-facing step was employed 50 mm and the aspect ratio was $AR = 12.5$. For the present experimental rig, the two-dimensional flow assumption is applicable to a reasonable accuracy, at least for much of the central portion of the test section. A AR ratio greater than 10 has been recommended by Brederode and Bradshaw (1978) to avoid significant side wall effects on the flow field near the center line of the channel. Therefore, the flow maintains a two dimensionality along the centerline of the test section.

Standard hot-wire technique was used with constant temperature anemometer (TSI-IFA300). A split-film probe (TSI model 1288) was used to measure the mean and fluctuating velocity statistics and the forward-flow time fraction γ_p for calculating the reattachment length. A total of 204800 voltage signal at each position was averaged and sent to a Pentium PC after the velocity signals were digitized by using a 4-channel A/D converter (UEI WIN-30DS). The A/D converter was equipped with a 12-bit A/D converter through the low-pass filter. All these instruments were

remote-controlled using an in-house LabVIEW program. A cut-off frequency was considered to be adequate for the measurements in turbulent flow fields. This cut-off frequency for measuring the turbulent properties was fixed at 5 kHz. The forward-flow time fraction was at 100 Hz. A sampling frequency was fixed at 10 kHz and 200 Hz for above two cases, respectively. The frequency response characteristics of the hot-wire probes were examined by square wave test (20 ~ 30) kHz.

Pressure fluctuations measurement

The PVDF film is suitable for sensing small pressure fluctuations due to the wide dynamic range and large piezoelectric constant of the transparent semicrystalline polymer film. Figure 1 shows an array of sensors, where 4×10 arrays of circular electrodes are plated in the area of $24\text{mm} \times 40\text{mm}$. The diameter of these circular electrodes is 3mm, and the spacing between centers of each electrode is 6mm.

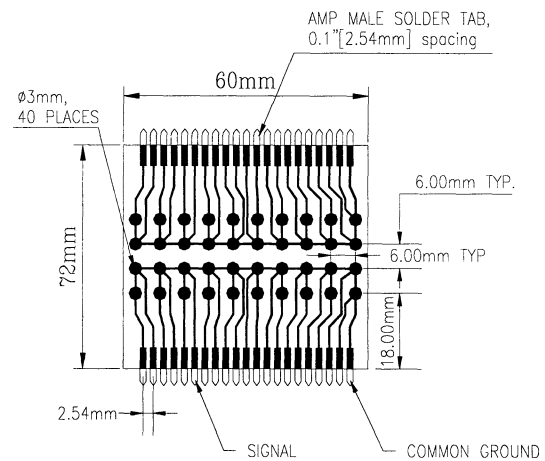


Figure 1. PVDF sensor used in this study

The frequency response of this sensor is examined by using a reference microphone. The PVDF signal is very small compared with the reference microphone signal. In addition, a peak noise is detected in the PVDF signal near 60Hz. For a robust sensor development, a primary concern is the appropriate remedy to compensate for the PVDF frequency response. In order to compensate for the frequency response of the sensor, a linear modeling of pressure measurement system was performed, and the transfer function of the sensor was estimated. The time history of the unsteady pressure was then reconstructed from the output of the sensor by using this transfer function. Details regarding the data reconstruction are given in Lee and Sung (1999).

Figure 3 represents the signal reconstruction in the case of the band-limited white noise input, which has the same conditions as that of Fig. 2. The autospectrum of the reconstructed signal in Fig. 3 shows a good agreement with that of the reference signal over most frequency bands. If we compare this output with the preceding figure (Fig. 2), where

the large discrepancy is exhibited, the present agreement is quite remarkable.

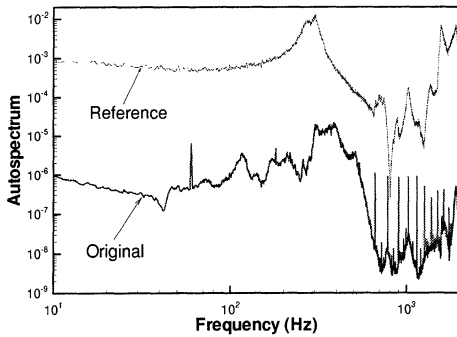


Figure 2. Comparison of autospectra from reference microphone output and PVDF output

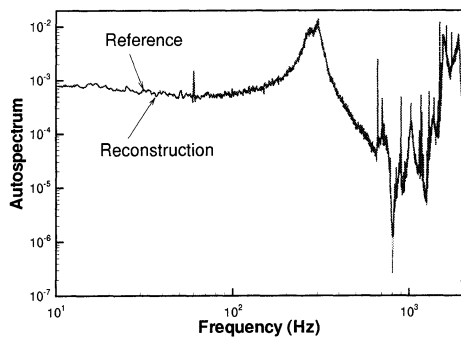


Figure 3. Result of white noise signal reconstruction

The successful reconstruction in the frequency domain indicates that, by utilizing the present signal reconstruction method, the PVDF sensor is promising in estimating the spectral energy distribution as well as the total energy of the pressure fluctuations.

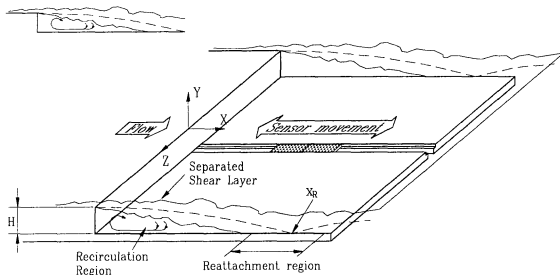


Figure 4. PVDF sensor installation

The PVDF sensor was installed in the streamwise slot of the test section, as shown in Fig. 4. By employing 32-channel charge amplifiers (Kistler Type 5017), 32 unsteady signals were sampled simultaneously with the rate of 2kHz. Prior to A/D conversion, a lowpass filter option with the cutoff frequency of 1kHz was used as an anti-aliasing filter.

RESULTS AND DISCUSSION

Flow field measurements

In the present experiment, the Reynolds number $Re_H = 33,000$ is selected, which coincides with the Reynolds number in the experiment of Chun and Sung (1996). Comparison of the present experimental results with those in the earlier work of Chun and Sung (1996) shows a reasonable agreement between them.

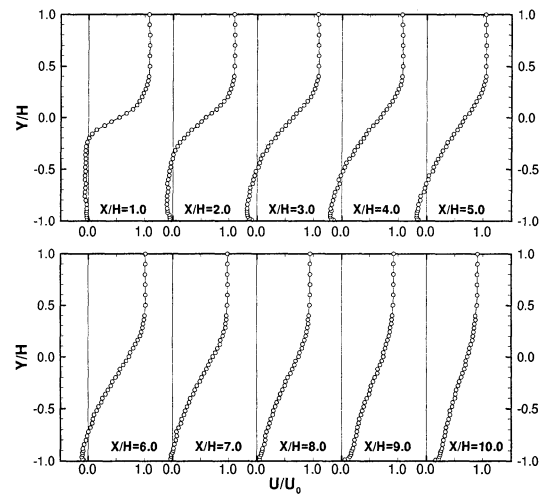


Figure 5. Streamwise mean velocity profiles

Among the various data representing the backward-facing step flow, the reattachment length x_R is frequently used as a representative quantity in a time-mean sense. In order to find the reattachment length, the forward-flow time fraction γ_p in the vicinity of the wall ($y/H = -0.98$) was measured by using a split film probe (TSI model 1288). The time-mean reattachment position x_R could be defined as the point, where the forward-flow time fraction has the value of $\gamma_p = 0.5$. Measured forward-flow time fraction reveals that the reattachment length x_R is equal to $7.4H$, which shows a close resemblance with $x_R = 7.8H$ in Chun and Sung (1996).

A detailed measurement was then performed in the several locations along the test section $1.0 \leq x/H \leq 10.0$. Figure 5 and Figure 6 give profiles of the streamwise mean velocity and the streamwise turbulence intensity, respectively. In Fig. 5, the existence of recirculation zone is clearly discernible. The presence of local maxima in the turbulence intensity profile and its broadening with respect to the streamwise direction clarify the growth behavior of separated shear layer.

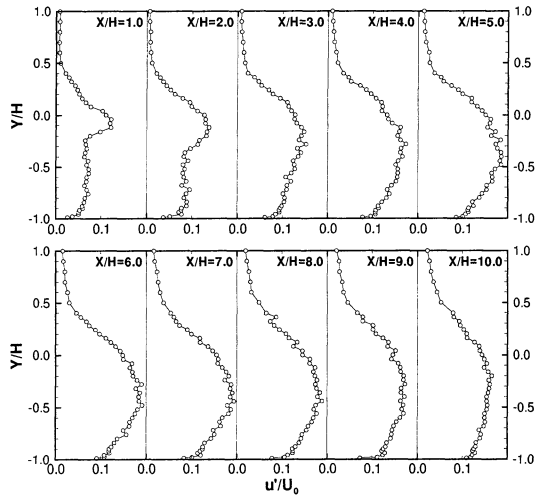


Figure 6. Streamwise turbulence intensity profiles

Pressure fluctuations measurements

RMS and spectrum. Figure 7 shows the streamwise distribution of rms pressure fluctuations, normalized by the inflow dynamic pressure ($q = \rho U_0^2 / 2$), as a function of downstream location. In this figure, the rms values begin to rise rapidly at about $x/h = 4.5$. The mean pressure coefficient (C_p) also begins to increase (see Fig. 8 of Chun and Sung, 1996). It is noteworthy that the increased level of rms value is closely correlated with the mean pressure recovery. Govinda Ram and Arakeri (1990) pointed out exactly the same relation.

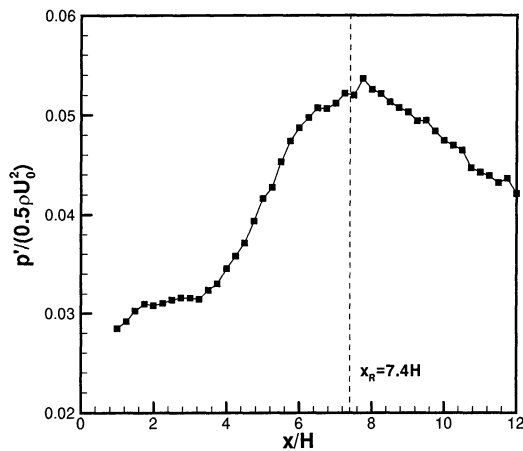


Figure 7. RMS distribution of pressure fluctuations

Devenport and Sutton (1991) identified the large-scale velocity fluctuations in the near-wall region of separated and reattaching flows, which is driven by pressure gradient

fluctuations imposed by the separated shear layer. The definite interrelation between the rms pressure and the mean pressure gradient suggests that the pressure fluctuations are mainly generated by unsteadiness imposed by the shear layer.

As flow goes downstream, the rms value reaches a maximum near the reattachment point ($x_R = 7.4H$), which has been reported by many researchers (Cherry et al., 1984; Kiya and Sasaki, 1983; Mabey, 1972). After reattachment, the rms value decreases slowly, and this is related to the lack of free shear layer activity. Furthermore, the slow reduction implies a long persistence of large-scale vortical motion after reattachment, as indicated by Farabee and Casarella (1986). They identified the deviation of pressure spectrum from the equilibrium boundary layer state as far as 72 step heights downstream of the step.

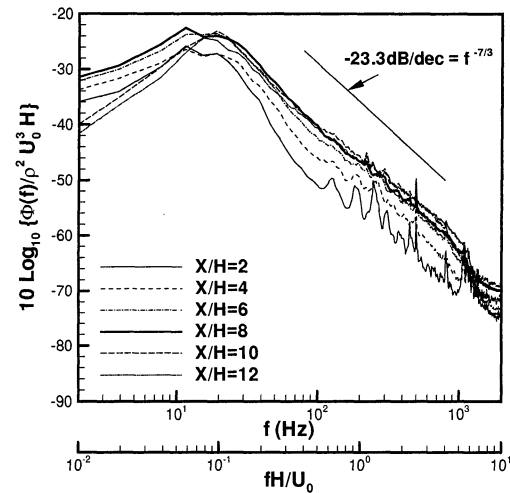


Figure 8. Frequency spectra of pressure fluctuations

In Fig. 8, the pressure autospectra measured at various locations are displayed. At $x/H=2$, compared with other locations, the spectrum level is generally low, except the very low frequency ($fH/U_0 \sim 0.015$). When rescaled with the reattachment length x_R , as Mabey (1972) proposed, the aforementioned nondimensional frequency $f x_R / U_0 \sim 0.015$ coincides with the flapping frequency (Eaton and Johnston, 1981). Cherry et al. (1984) also indicates the relative dominance of very low frequency component in this region, close to separation point.

Throughout all locations, the pressure spectrum reaches a maximum at $fH/U_0 \sim 0.10$, which is equivalent to the frequency of large-scale vortical structure, i.e., $f x_R / U_0 \sim 0.75$ (Driver et al., 1987). In addition, as x/H increases, the high frequency components continue to increase, and the fall-off rate approaches asymptotically $-7/3$ power. George et al. (1984) developed a spectral model for turbulent pressure fluctuations by Fourier transforming the solution of Poisson equation for a free shear flow with constant mean shear. Between the two kinds of source terms of the Poisson equation, they addressed that the turbulence-turbulence

interaction term governs the $-7/3$ fall-off rate and dominates the high-wavenumber region. The same fall-off rate in Fig. 8 gives some conclusion that, in the later part of recirculation region ($4.0 \leq x/H \leq 8.0$), the pressure fluctuations are largely attributable to the separated shear layer. Furthermore, the aforementioned slow relaxation process supports a close resemblance of spectra after reattachment. This suggests a relative importance of the shear-layer-originated spatio-temporal characteristics over boundary-layer-like features.

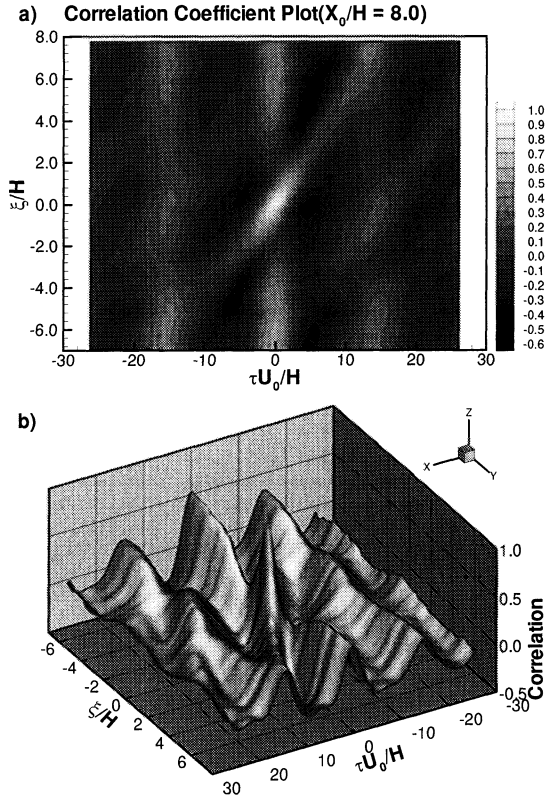


Figure 9. Cross correlation coefficient of pressure fluctuations with $x_0=8h$

Space-time cross correlation. The cross correlation coefficient $\rho_{pp}(\xi, \tau)$ of pressure fluctuations between two sensors (at various separation distance, ξ and time delay τ) is defined as follows.

$$\rho_{pp}(\xi, \tau) = \frac{R_{pp}(\xi, \tau)}{\sqrt{p_1^2(x_0, \tau)} \sqrt{p_2^2(x_0 + \xi, t + \tau)}}$$

$$R_{pp}(\xi, \tau) \equiv p_1(x_0, \tau) p_2(x_0 + \xi, t + \tau)$$

Since there exist different flow regimes such as recirculation and reattachment region, the flow should be considered to be inhomogeneous. Therefore, the correlation coefficient is also a function of the origin, x_0 .

In Fig. 9 a), the correlation coefficient at $x_0=8h$ is illustrated in the form of isocorrelation contour plot. A brief glance at Fig. 9 a) discloses a clear demarcation of the region of high correlation, which is biased with a nearly constant slope in (τ, ξ) -plane. This nonzero, finite slope provides an evidence of the convection of coherent eddies. It is also obvious that, as the distance between the sensors increases, the eddies gradually lose their identities. Furthermore, it can be found that if the sensor separation distance ξ exceeds $\pm 2.5h$, the “convective” correlation region almost disappears. A “stationary” region emerges, because the maximum correlation occurs at nearly “zero” time delay.

A more instructive method for plotting data is attempted in Fig. 9 b), where a three-dimensional plot of the correlation coefficient is exhibited. A “convective ridge” of the high correlation is very similar in character to that found in the measurements of Willmarth and Wooldridge (1962). In addition, there are “stationary ridges” with the time interval $\Delta\tau U_0/H \sim 16.0$ between them. Whether this “stationary ridge” is unique flow feature is open to some debate at this moment. This is because no similar phenomena have been reported so far.

Coherence function. The transition from the space-time cross correlation $R_{pp}(\xi, \tau)$ to the cross-spectrum $\Phi(\xi, f)$ gives an alternative viewpoint, which is defined by Fourier transforming the cross correlation $R_{pp}(\xi, \tau)$ with respect to τ . In general, since the cross-spectrum is a complex quantity, the coherence function $\Gamma(\xi, f)$ is employed for the convenience of the data representation.

$$\Gamma(\xi, f) = \frac{|\Phi(\xi, f)|}{\sqrt{\Phi_{p_1}(f) \Phi_{p_2}(f)}}$$

In the above, $\Phi_{p_1}(f)$ and $\Phi_{p_2}(f)$ denote the autospectra at points x_0 and $x_0 + \xi$, respectively. In this study, the coherence is obtained for $x_0=8h$, $0 \leq \xi/h \leq 8$.

Figures 10 a) and b) show the coherence function with $x_0=8h$ in the form of 2D and 3D plots, respectively. A global inspection reveals that the coherence decays, as the sensor separation distance and frequency increase. In other words, a monotonic decay with respect to $\omega\xi/U_0$, which is the celebrated “Corcos’ model”, seems to govern the spatial behavior of pressure field.

The high coherence regions are observed near $\xi/h=3.0$ and $\xi/h=6.0$, which are separated from the “main lobe” in Fig. 10 a). The “undulations” in Fig. 10 b) preclude the legitimacy of boundary-layer-type decaying models. The frequency of these “undulations” is $fH/U_0 \sim 0.10$, which coincides with the frequency of large-scale vortical structure. Furthermore, it is notable that the location of undulations, $\xi/h=3.0$, implies the average distance between large-scale vortices.

This behavior of coherence function has never been reported so far. Farabee and Casarella (1986) made measurement only with relatively small separations of $\xi/h=1.0$ and 1.5 . Since they assumed a dependence of similarity variable such as $\omega\xi/U_0$, they could not resolve large-scale

pressure behavior. Only decaying character of pressure field was found.

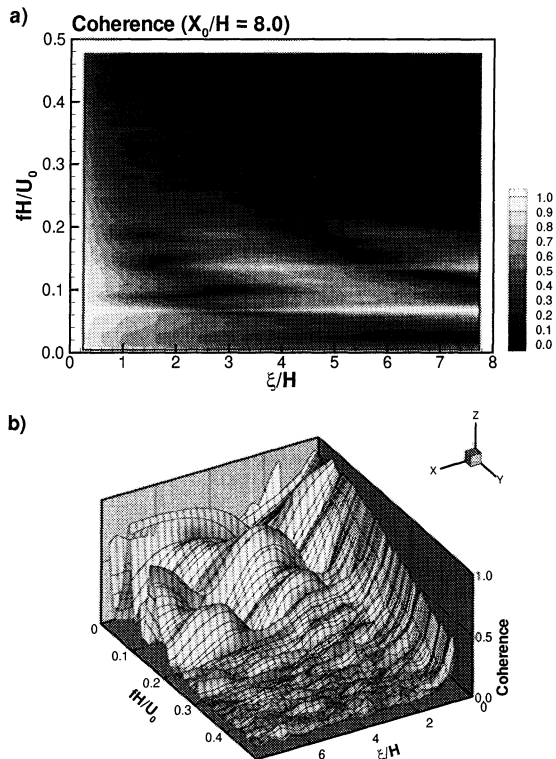


Figure 10. Coherence function of pressure fluctuations

CONCLUSIONS

Surface pressure fluctuations in the flow over a backward-facing step have been measured. The Reynolds number based on the step height (H) was $Re_H=33,000$. A new type of an array of pressure sensors, composed of PVDF (polyvinylidene fluoride), was utilized for the examination of spatio-temporal features of pressure field. Distributions of the rms pressure fluctuations as well as pressure autospectra, cross correlation coefficient and coherence function were measured at various locations near reattachment point. One-point statistics, such as rms distribution and autospectra shows reasonable spatial and spectral behaviors, compared with existing data. Two-point statistics reveals that there exists a large-scale, convective spatial structure, which is coherent over several step heights. This finding is consistent with the existence of well-known vortical structures in this type of flow.

REFERENCES

- Brederode, V., and Bradshaw, P., 1978, "Influence of the side walls on the turbulent center-plane boundary-layer in a squar duct," *J. Fluids Eng.*, vol.100, pp.91-96
- Cherry, N. J., Hillier, R., and Latour, M. E. M. P., 1984, "Unsteady measurements in a separated and reattaching flow," *J. Fluid Mech.*, vol.144, pp.13-46
- Choi, H., and Moin, P., 1990, "On the space-time characteristics of wall-pressure fluctuations," *Phys. Fluids* vol. A2, pp.1450-1460
- Chun, K. B., and Sung, H. J., 1996, "Control of turbulent separated flow over a backward-facing step," *Exp. Fluids*, vol.21, pp.417-426
- Devenport, W. J., and Sutton, E. P., 1991, "Near-wall behavior of separated and reattaching flows," *AIAA J.*, vol.29, pp.25-31
- Driver, D. M., Seegmiller, H. L., and Marvin, J. G., 1987, "Time-dependent behavior of a reattaching shear layer," *AIAA J.*, vol.25, pp.914-919
- Eaton, J. K., and Johnston, J. P., 1981, "A review on research on subsonic turbulent flow reattachment," *AIAA J.*, vol.19, pp.1093-1100
- Farabee, T. M., and Casarella, M. J., 1986, "Measurements of fluctuating wall pressure for separated/reattached boundary layer flows," *J. Vibration, Acoustics, Stress, and Reliability in Design*, vol.108, pp.301-307
- Farabee, T. M., and Casarella, M. J., 1991, "Spectral features of wall pressure fluctuations beneath turbulent boundary layer," *Phys. Fluids*, vol.A3, pp.2410-2420
- George, W. K., Beuther, P., D., and Arndt, R., E., A., 1984, "Pressure spectra in turbulent free shear flows," *J. Fluid Mech.*, vol.148, pp.155-191
- Govinda Ram, H. S., and Arakeri, V. H., 1990, "Studies on unsteady pressure fields in the region of separating and reattaching flows," *J. Fluids Eng.*, vol. 112, pp.402-408
- Kiya, M., and Sasaki, K., 1983, "Structure of a turbulent separation bubble," *J. Fluid Mech.*, vol.137, pp.83-113
- Kiya, M., and Sasaki, K., 1985, "Structure of large-scale vortices and unsteady reverse flow in the reattaching zone of a turbulent separation bubble," *J. Fluid Mech.*, vol.154, pp.463-491
- Lee, I., and Sung, H. J., 1999, "Development of an array of pressure sensors with PVDF film," *Exp. Fluids*, vol.26, pp.27-35
- Mabey, D. G., 1972, "Analysis and Correlation of Data on Pressure Fluctuations in Separated Flow," *J. Aircraft*, vol.9, pp.642-645
- Schewe, G., 1983, "On the structure and resolution of wall-pressure fluctuations associated with turbulent boundary-layer flow," *J. Fluid Mech.*, vol.134, pp.311-328
- Willmarth, W. W., and Wooldridge, C. E., 1962, "Measurement of the fluctuating pressure at the wall beneath a thick boundary layer," *J. Fluid Mech.*, vol.14, pp.187-210